Extended Finnis–Sinclair potential for bcc and fcc metals and alloys

X D Dai, Y Kong, J H Li and B X Liu[1]

Advanced Materials Laboratory, Department of Materials Science and Engineering,
Tsinghua University, Beijing 100084, People's Republic of China

E-mail: dmslbx@tsinghua.edu.cn

Abstract
We propose an extended Finnis–Sinclair (FS) potential by extending the
repulsive term into a sextic polynomial for enhancing the repulsive interaction
and adding a quartic term to describe the electronic density function. It turns
out that for bcc metals the proposed potential not only overcomes the 'soft'
behaviour of the original FS potential, but also performs better than the modified
FS one by Ackland *et al*, and that for fcc metals the proposed potential is able
to reproduce the lattice constants, cohesive energies, elastic constant, vacancy
formation energies, equations of state, pressure–volume relationships, melting
points and melting heats. Moreover, for some fcc–bcc systems, e.g. the Ag–
refractory metal systems, the lattice constants, cohesive energies and elastic
constants of some alloys are reproduced by the proposed potential and are quite
compatible with those directly determined by *ab initio* calculations.

(Some figures in this article are in colour only in the electronic version)

1. Introduction

Since the 1980s, a variety of empirical *n*-body potentials have been introduced and employed
to study the bulk, surface and cluster properties of metals [1–4]. Although the introduced
potentials, such as the tight-binding approach based on the second moment approximation [5],
the so-called embedded atom method (EAM) [6] and the Finnis–Sinclair (FS) potential [7],
have different forms in their details, they have similar formulations, which represent the total
potential energy of a system as a sum of a pairwise interaction term and an *n*-body one. Among
these potentials, the scheme developed by Finnis and Sinclair based on a second-moment
approximation to the tight-binding density of states has a simply analytic form and has been
shown to give very good results in simulations of point defects, grain boundaries, surfaces and
amorphization transitions for metals and alloys [8–12]. Nonetheless, in the applications of

---

[1] Author to whom any correspondence should be addressed.

FS potential, researchers have found some shortcomings of the potential. One is that the FS potential is systematically too 'soft', as it moves away from the equilibrium volume [13, 14]. To overcome such a shortcoming, Ackland and Thetford have proposed to add a 'core' into the repulsive term in FS formalism to enhance the short-range atomic interactions, thus improving the pressure–volume relationships for some bcc metals, i.e. V, Nb, Ta, Mo and W [14]. A similar modification has also been proposed by Rebonato *et al* [13]. It is noted, however, that the modified potential is too stiff compared with the universal equation of state, i.e. the Rose equation [15], when the distance is less than the equilibrium one. Another shortcoming is that the FS potential has some difficulty in satisfactorily reproducing the static physical properties for some fcc metals, especial for noble metals. In this regard, Ackland *et al* have pointed out that the problem might be attributed to the electronic structure difference between the bcc and fcc metals and proposed another formalism for noble metals and nickel under the framework of FS potential [16]. Nonetheless, the proposed formalism is more complex than the original FS formalism, as one of the potential parameters is determined by fitting the pressure–volume relationship, which is rather difficult to obtain experimentally when the pressure is very high.

We propose, in the present study, an extended FS potential, which also has a simply analytic form and can be widely used to calculate many properties of bcc and fcc metals and alloys. We will introduce the proposed extended FS potential through the following four steps. First, the detailed formalism of extended FS potential is introduced. Second, we will show how extended FS potential overcomes the first shortcoming of FS potential through reproducing the equation of state for some bcc metals, and how extended FS potential performs better than the previously modified FS potential by Ackland *et al*. Third, extended FS potential is applied in reproducing some properties of six selected fcc metals, i.e. Cu, Ag, Au, Ni, Pd and Pt, such as the lattice constants, cohesive energies, elastic constants, equations of state, pressure–volume relationships, melting points and melting heats. Fourth, the extended FS potential is applied to four fcc–bcc systems, i.e. the Ag–refractory metal systems, to calculate lattice constants, cohesive energies and elastic constants of the respective alloys in the systems.

2. The model of extended FS potential

According to EAM or FS formalism, the total energy of a system is given by

$$U_{\text{tot}} = \frac{1}{2} \sum_{ij} V(r_{ij}) - \sum_i f(\rho_i). \tag{1}$$

The first term in equation (1) is the conventional central pair-potential summation, which is expressed by a quartic polynomial in original FS formalism [7] and by an exponential form in Johnson's EAM potential [17]. In the present study, we propose to use a sextic polynomial for improving the repulsive interaction between the atoms and the extended term is expressed by

$$V(r) = \begin{cases} (r-c)^2(c_0 + c_1 r + c_2 r^2 + c_3 r^3 + c_4 r^4), & r \leqslant c \\ 0, & r > c \end{cases} \tag{2}$$

where c is a cut-off parameter assumed to lie between the second and third neighbour atoms. c_0, c_1, c_2, c_3 and c_4 are the potential parameters to be fitted. The second term in equation (1) is the n-body term. Based on a second-moment approximation to the tight-binding density of states, the embedding function f can be expressed by

$$f(\rho_i) = \sqrt{\rho_i}, \tag{3}$$

where, according to the linear superposition approximation, the host electronic density ρ_i can be written as the sum of the electronic density functions $\phi(r_{ij})$ of the individual atoms i, i.e.

$$\rho_i = \sum_{j \neq i} A^2 \phi(r_{ij}). \tag{4}$$

In the original FS potential, the electronic density function is a quadratic term. In the present study, we propose to add a quartic term in the electronic density function to improve the description of the electronic structure of metals. The electronic density function is expressed by

$$\phi(r) = \begin{cases} (r-d)^2 + B^2(r-d)^4, & r \leqslant d \\ 0, & r > d. \end{cases} \tag{5}$$

Note that the term $B^2(r-d)^4$ is added in equation (5) to improve the performance of the potential in describing the electronic density of metals, especially of fcc metals. In equation (5), the cut-off parameter d is also assumed to lie between the second and third neighbour atoms. Apparently, the proposed extended FS potential is still a simple short-range potential, and when the potential parameters, c_3, c_4 and B, are all set to be zero, the extended FS potential turns into the original FS formalism. Consequently, the extended FS potential could work for whatever original the FS formalism could do for bcc metals and is expected to work well for fcc metals as well as for some bcc–fcc systems.

3. Application for bcc metals

Since it has been demonstrated that the FS potential is a reliable and effective scheme for treating many issues of pure bcc metals, the extended FS potential should also work well in the same aspects. In table 1, we list some basic physical properties reproduced from extended FS potentials for six selected bcc metals, i.e. Fe, V, Mo, Nb, Ta and W, and for comparison the corresponding experimental values are also listed. From the table, one sees clearly that the reproduced lattice constants, cohesive energies, elastic constants and vacancy formation energies of the selected metals are in good agreement with their respective experimental values, showing the excellent performance of extended FS potential for bcc metals. In the following sub-sections, we will use the extended FS potential to calculate some other physical properties of bcc metals so as to further validate the performance of the extended FS potential for bcc metals.

3.1. Structural stability and equation of state

In the fitting procedure, we do not consider whether the bcc crystal structure is more stable than an fcc or hcp one. However, it is known that the global stability is very important to test the reliability of a potential. Based on the newly constructed extended FS potentials, the cohesive energies and lattice constants have been calculated for the six selected bcc metals and the results are listed in table 2. From table 2, one can clearly see that the cohesive energy of each bcc structure is greater than that of its corresponding fcc or hcp structure, reflecting well the fact that the equilibrium states of the six metals are bcc structures. Interestingly, the cohesive energies for fcc and hcp structures are exactly the same for all the six metals in table 2. In fact, when the cut-off parameter of a potential lies between the second and third neighbour atoms, the potential is not able to distinguish the difference between an fcc structure and an ideal hcp structure, leading to the same calculated cohesive energy for both structures listed in table 2. To

Table 1. The comparison between the properties reproduced by the extended FS potential and the experimental values for pure Fe, V, Mo, Nb, Ta and W.

		Fe	V	Mo	Nb	Ta	W
a (Å)	Reproduced	2.870	3.030	3.1472	3.300	3.300	3.160
	Experimental[a,b]	2.87	3.03	3.1472	3.30	3.30	3.16
E_c (eV)	Reproduced	4.273	5.339	6.818	7.572	8.084	8.916
	Experimental[a,b]	4.28	5.31	6.82	7.57	8.10	8.90
C_{11} (Mbar)	Reproduced	2.263	2.240	4.631	2.470	2.308	5.308
	Experimental[a,b]	2.26	2.29	4.637	2.47	2.663	5.32
C_{12} (Mbar)	Reproduced	1.406	1.175	1.589	1.347	1.435	2.058
	Experimental[a,b]	1.40	1.21	1.578	1.35	1.582	2.049
C_{44} (Mbar)	Reproduced	1.155	0.448	1.087	0.287	0.913	1.626
	Experimental[a,b]	1.16	0.444	1.092	0.287	0.874	1.631
E_v^f (eV)	Reproduced	1.861	2.123	2.555	2.746	2.905	3.707
	Experimental	1.79[c]	2.20[d]	3.10[e]	2.75[e]	2.18[f]	3.95[g]
			Potential parameters				
A (eV Å^{-1})		0.931 312	1.922 282	1.848 648	2.999 182	2.702 029	1.885 948
d (Å)		4.05	3.69	4.1472	3.90	4.15	4.41
c (Å)		2.96	3.70	3.2572	4.07	3.77	3.25
c_0 (eV Å^{-2})		26.270 34	23.691 18	47.980 66	25.575 48	30.911 55	48.527 96
c_1 (eV Å^{-3})		−24.401 09	−25.758 98	−34.099 24	−26.842 73	−26.579 02	−33.796 21
c_2 (eV Å^{-4})		6.957 871	9.393 983	5.832 293	9.903 115	6.651 629	5.854 334
c_3 (eV Å^{-5})		−0.303 077	−1.028 748	0.017 494	−1.297 269	0.007 0699	−0.009 8221
c_4 (eV Å^{-6})		−0.085 092	−0.039 966	0.020 393	0.014 2888	−0.128 597	0.033 338
B (Å^{-2})		0	0	0	0	0	0

[a] Reference [18]; [b] Reference [19]; [c] Reference [20]; [d] Reference [21]; [e] Reference [22]; [f] Reference [23]; [g] Reference [24].

Table 2. The calculated cohesive energies (the unit is in eV) of pure Fe, V, Mo, Nb, Ta and W in three simple crystalline structures (bcc, fcc and ideal hcp).

	bcc		fcc		hcp	
	a	E_c	a	E_c	a	E_c
Fe	2.870	4.2734	3.600	4.2706	2.546	4.2706
V	3.030	5.3393	3.871	5.1067	2.737	5.1067
Mo	3.1472	6.8176	3.8482	6.5667	2.7212	6.5667
Nb	3.300	7.5723	4.219	7.2472	2.983	7.2472
Ta	3.300	8.0601	4.194	7.8788	2.965	7.8788
W	3.160	8.9164	3.898	8.7630	2.756	8.7630

distinguish the energy difference between the two structures, a longer cut-off parameter, e.g. at least greater than the distance of the third neighbour atom, should be adopted.

As mentioned above, the FS potential has an apparent shortcoming when treating the pressure–volume relationship of some bcc metals, i.e. the potential is too 'soft' when it moves away from the equilibrium volume. In order to validate extended FS potential in this aspect, we calculate the equations of state of the six bcc metals based on the potentials and plot them in figure 1. For comparison, the equations of state derived from the Rose equation, FS potential
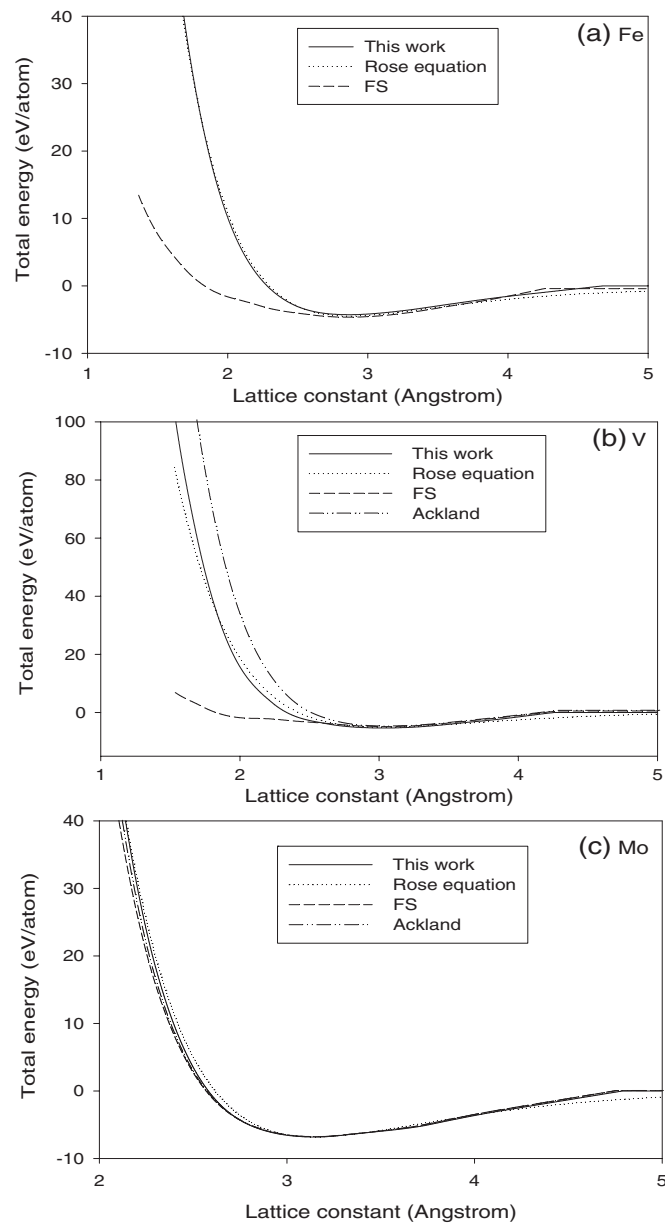
Figure 1. Equations of state derived from extended FS potentials (solid line), Rose equation (dotted line), FS potentials (dashed line) and Ackland's improved FS potentials (dash–dot–dot line), respectively, for (a) Fe, (b) V, (c) Mo, (d) Nb, (e) Ta and (f) W.

and Ackland's modified FS potential, respectively, are also plotted in figure 1. It is known that the Rose equation, which is deduced from many experimental pressure–volume data and shows a good agreement with the experimental data, can be regarded as the universal equation of state for most of the metals [15]. From figure 1, one sees that compared with the Rose equation, the FS potential really shows a too 'soft' behaviour when it treats the cases of Fe, V, Nb and Ta. In fact, Finnis and Sinclair recognized such a shortcoming when they published their formalism
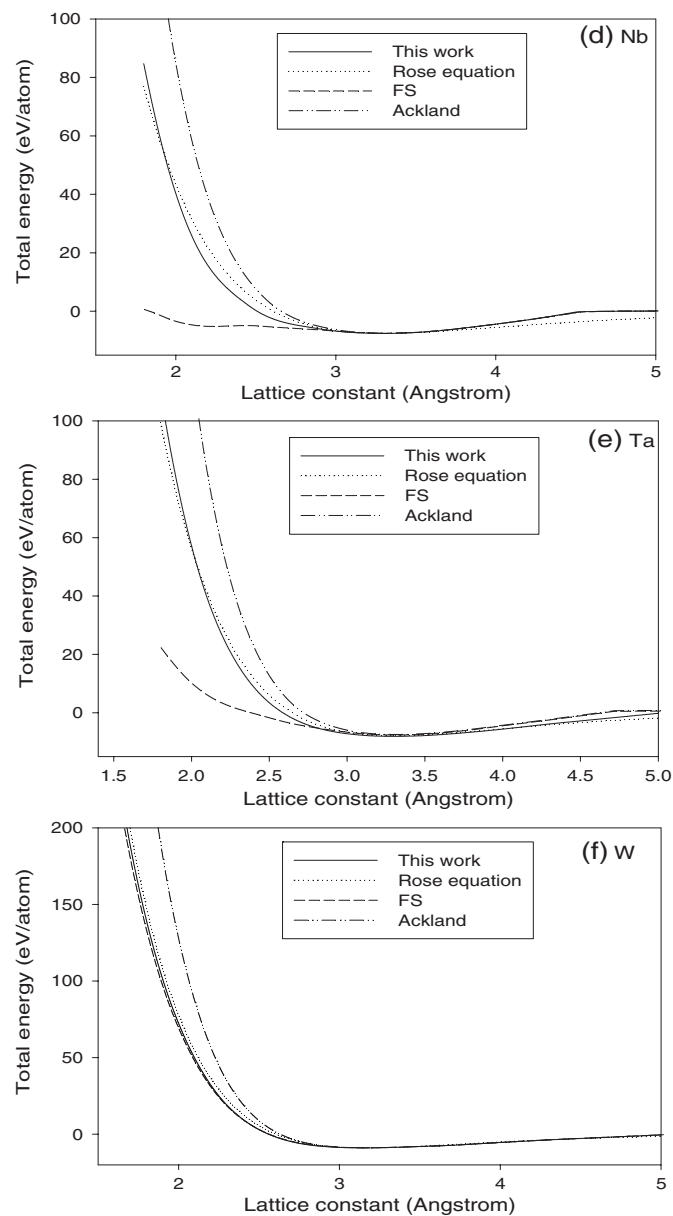
Figure 1. (Continued.)

in 1984, and in order to improve the pressure–volume relationship of Cr and Fe they added a term in the electronic density function, which is expressed by [7]

$$\phi(r) = \begin{cases} (r-d)^2 + B(r-d)^3/d, & r \leqslant d \\ 0, & r > d. \end{cases} \qquad (6)$$

The added term indeed improves the pressure–volume relationship of Cr; however, as shown in figure 1(a), the potential of Fe is still too 'soft' when the lattice constant has a small value. Three years later, Ackland *et al* proposed to add a 'core' to the repulsive term in the FS formalism to

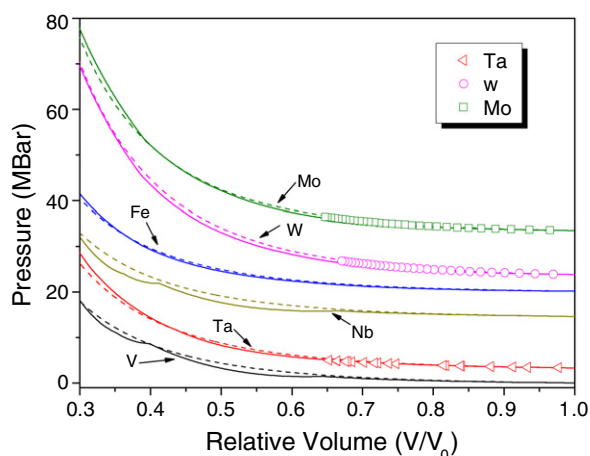**Figure 2.** The pressure versus volume relationships for six bcc metals, i.e. Fe, V, Mo, Nb, Ta and W. The solid curves are from extended FS potentials, the dashed curves are from the Rose equation, and the scattered dots are from experiments. The experimental data of Ta are from [25], and those of Mo and W are from [26].

enhance the short-range atomic interactions, thus improving the pressure–volume relationships for some bcc metals, i.e. V, Nb, Ta, Mo and W [14]. The 'core' is an exponential term and is expressed by

$$g(r) = \beta(b_0 - r)^3 \exp(-\alpha r). \tag{7}$$

From figure 1, one sees that Ackland's modified FS potential has indeed overcome the 'soft' character of the original FS potential when the lattice constant is less than the equilibrium one, yet is too stiff when compared with the Rose equation. Inspecting the equations of state derived from the extended FS potential for six selected bcc metals, i.e. Fe, V, Mo, Nb, Ta and W, in figure 1, one sees that the extended FS potential not only overcomes the 'soft' shortcoming of the original FS formalism, but also shows good agreement with those derived from the Rose equation. In other words, the treatment to the repulsive term proposed in the present study is quite reasonable and the extended FS potential does perform better than Ackland's modified one.

3.2. Pressure–volume relationship

During simulation, such as MD simulation, the volume of a simulation model frequently changes with the imposed pressure. The pressure–volume relationship is therefore very important for a potential while applying to perform simulations. Accordingly, we calculate the relationships of the pressure versus volume for the six selected bcc metals based on extended FS potentials and compared the results with those obtained from the Rose equation and experiments, respectively, in figure 2. One sees from figure 2 that for Fe, Mo, Ta and W the calculated results between extended FS potentials and the Rose equation are in good agreement even at a very small volume, and that for V and Nb the calculated results from extended FS potentials are a little smaller than those from the Rose equation at small volume. More importantly, the calculated results of Mo, Ta and W are in good agreement with the experimental values.

Table 3. The melting points and melting heats for six selected bcc metals. The experimental data are from [19].

		Fe	V	Mo	Nb	Ta	W
Melting point	MD	2100	2500	3300	3000	3450	4500
(K)	Expt	1811	2202	2895	2750	3293	3695
Melting heat	MD	17.25	19.72	30.69	23.69	25.22	29.71
(kJ mol^{-1})	Expt	13.80	20.90	32.00	26.40	31.60	35.40

3.3. Melting point and melting heat

Reasonably predicting the basic thermodynamics properties of metals is another important point for a relevant *n*-body potential; we therefore validate the proposed extended FS potential by calculating the melting points of the six selected bcc metals. Based on extended FS potentials, molecular dynamics simulations are carried out with solid solution models to determine the melting points of the metals [27]. The knowledge from phase transition theory indicates that at the melting point the heat of formation has an apparent change, which corresponds to the melting heat. Accordingly, during the MD simulations, the heat of formation of the solid solution model is monitored with variation of temperature to determine the melting points of metals. The melting points and the melting heats determined by MD simulations as well as their corresponding experimental values for the six selected bcc metals are all listed in table 3. One sees from the table that the calculated melting points are in reasonable agreement with the experimental values with a maximum error of 21.78%. For the melting heats, the calculated values are considered to be compatible with the experimental values with a maximum error of about 25.00%. In short, the proposed extended FS potential is therefore quite reasonable to describe the thermodynamic behaviour of bcc metals.

4. Application for fcc metals

The proposed extended FS potential can also be used to treat the cases of fcc metals. Table 4 lists the potential parameters for six selected fcc metals, i.e. Cu, Ag, Au, Ni, Pd and Pt, some properties of these metals reproduced from the extended FS potential, and their corresponding properties observed in experiments. One sees from the table that the reproduced values for Cu, Ag and Pt are in excellent agreement with the experimentally observed ones, with the largest root-square deviation (X_{rmx}) being less than 0.011%, and that the reproduced values for Au, Pd and Ni are also considered to match reasonably well with the experimental ones, with the largest X_{rmx} being around 5.82%. In fact, in reproducing the static properties of fcc metals, extended FS potentials work even better than the EAM potentials derived by both Foiles and Cai [31, 32], as in their cases the largest X_{rmx} was reported to be around 6.65% and the minimum X_{rmx} never went to zero. In the following sub-sections, we will further show the application of the extended FS potential to calculate some other properties of these fcc metals, such as the equation of state, pressure–volume relationship, melting point and melting heat.

4.1. Equation of state

Figure 3 displays the equations of state for the six fcc metals, i.e. Cu, Ag, Au, Ni, Pd and Pt, calculated from their extended FS potentials and the Rose equation, respectively. One sees from the figure that the results derived from extended FS potentials are in good agreement with those deduced from the Rose equation. The agreement is best for Cu, Ag, Au and Ni, and good for

Table 4. The comparison between the properties reproduced by the extended FS potential and the experimental values for pure Cu, Ag, Au, Ni, Pd and Pt.

		Cu	Ag	Au	Ni	Pd	Pt
a (Å)	Reproduced	3.610	4.090	4.080	3.520	3.890	3.920
	Experimental[a]	3.61	4.09	4.08	3.52	3.89	3.92
E_c (eV)	Reproduced	3.490	2.950	3.885	4.437	3.949	5.834
	Experimental[a]	3.49	2.95	3.81	4.44	3.89	5.84
C_{11} (Mbar)	Reproduced	1.684	1.240	1.923	2.450	2.271	3.470
	Experimental[a,b]	1.684	1.24	1.923	2.45	2.271	3.47
C_{12} (Mbar)	Reproduced	1.214	0.937	1.348	1.485	1.473	2.526
	Experimental[a,b]	1.214	0.937	1.631	1.40	1.761	2.51
C_{44} (Mbar)	Reproduced	0.754	0.461	0.438	1.182	0.764	0.764
	Experimental[a,b]	0.754	0.461	0.42	1.25	0.717	0.765
E_v^f (eV)	Reproduced	1.280	1.100	0.774	1.624	1.169	1.512
	Experimental	1.28[c]	1.1[c]	0.9[c]	1.60[d]	1.4[d]	1.5[c]
X_{rms} (%)		0	0	4.99	0.69	5.82	0.011
Potential parameters							
A (eV Å^{-1})		0.391 865	0.325 514	0.013 7025	0.982 477	0.049 9173	0.150 23
d (Å)		4.32	4.41	4.46	4.12	4.50	4.12
c (Å)		4.29	4.76	4.16	4.22	3.98	4.61
c_0 (eV Å^{-2})		10.187 24	10.681 2	44.968 58	13.282 76	23.600 65	31.501 62
c_1 (eV Å^{-3})		−12.820 33	−12.045 17	−55.128 26	−17.085 06	−28.240 54	−37.906 21
c_2 (eV Å^{-4})		6.176 587	5.203 072	25.846 57	8.262 515	13.116 04	17.481 37
c_3 (eV Å^{-5})		−1.341 391	−1.013 304	−5.445 922	−1.770 48	−2.785 318	−3.627 633
c_4 (eV Å^{-6})		0.109 842	0.074 2308	0.432 66	0.141 39	0.227 087	0.282 552
B (Å^{-2})		−0.881 096	−1.293 394	−53.963 0	0	10.684 04	9.3107

[a] Reference [18]. [b] Reference [28]. [c] Reference [29]. [d] Reference [30].

Pt and Pd. It should be noted that though we have not fitted the Rose equation as in the fitting procedure in the EAM scheme [17], the equations of state calculated by extended FS potentials for both bcc and fcc metals are all in agreement with those from the Rose equation. In other words, the proposed extended FS potential is excellent at describing the relationship between the total energy and lattice constant, even when the distance is far from an equilibrium state.

During MD simulation, the interatomic force deduced from the derivative of the total energy is a very important physical variable, which directly affects the simulation result. In general, for a curve of force versus distance, continuousness, no sharp fluctuations, and no odd points are all the basic features to insure obtaining the correct result. In figure 3, the derivative of total energy calculated from extended FS potentials for Cu, Ag, Au, Ni, Pd and Pt metals together with those deduced from the Rose equation are shown. From the figure, one sees that for all the studied metals the derivatives of total energy derived from the extended FS potential vary continuously and smoothly with the lattice constants, and that the calculated results are in good agreement with those derived from the Rose equation, implying the extended FS potential can reasonably describe the interaction in fcc metals.

4.2. Pressure–volume relationship

We also calculate the relationships of pressure versus volume for the six selected fcc metals based on their extended FS potentials and compare the results with those derived from the Rose
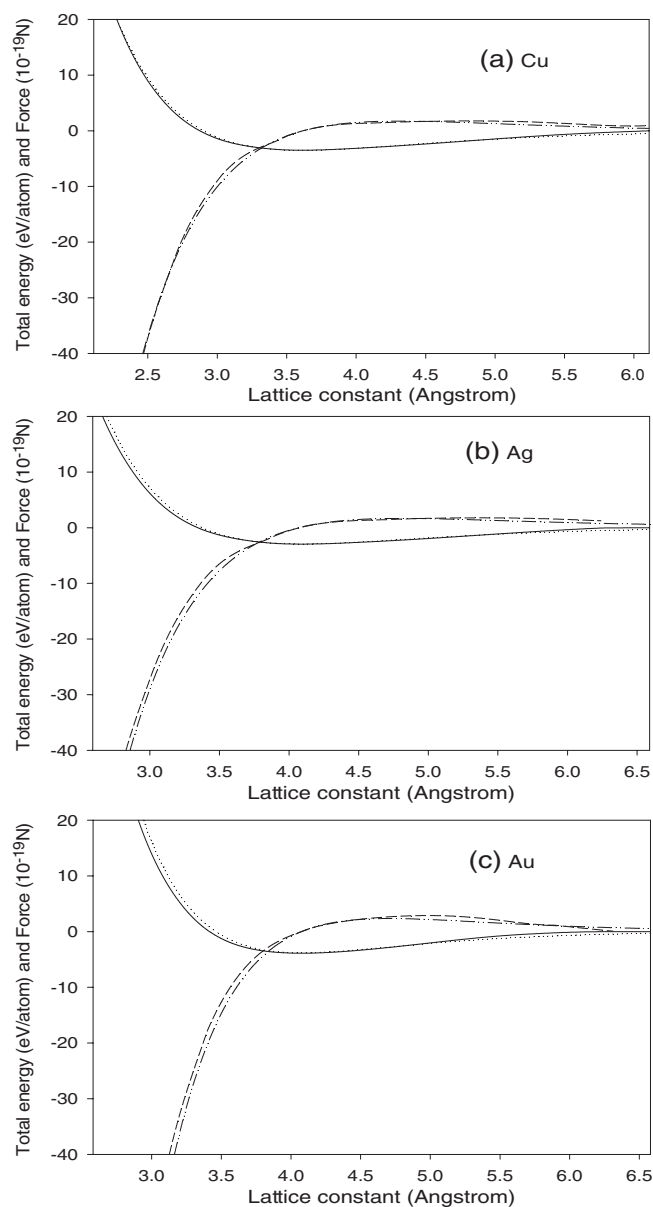
Figure 3. Equations of state and derivatives of energy for six fcc metals, i.e. (a) Cu, (b) Ag, (c) Au, (d) Ni, (e) Pd and (f) Pt. Solid lines and dotted lines are the total energies derived from extended FS potentials and the Rose equation, respectively. Dashed lines and dash–dot–dot lines are their derivatives with respect to the lattice constant, respectively.

equation in figure 4. One sees from the figure that for Cu, Ag, Ni and Pd the calculated results between the extended FS potential and the Rose equation are in good agreement even at a very small volume, and that for Au and Pt the calculated results from the extended FS potential are a little smaller than those from the Rose equation at small volume. In figure 5, the calculated results of Cu, Ag, Au, Pt and Pd have been compared with their respective experimental values.
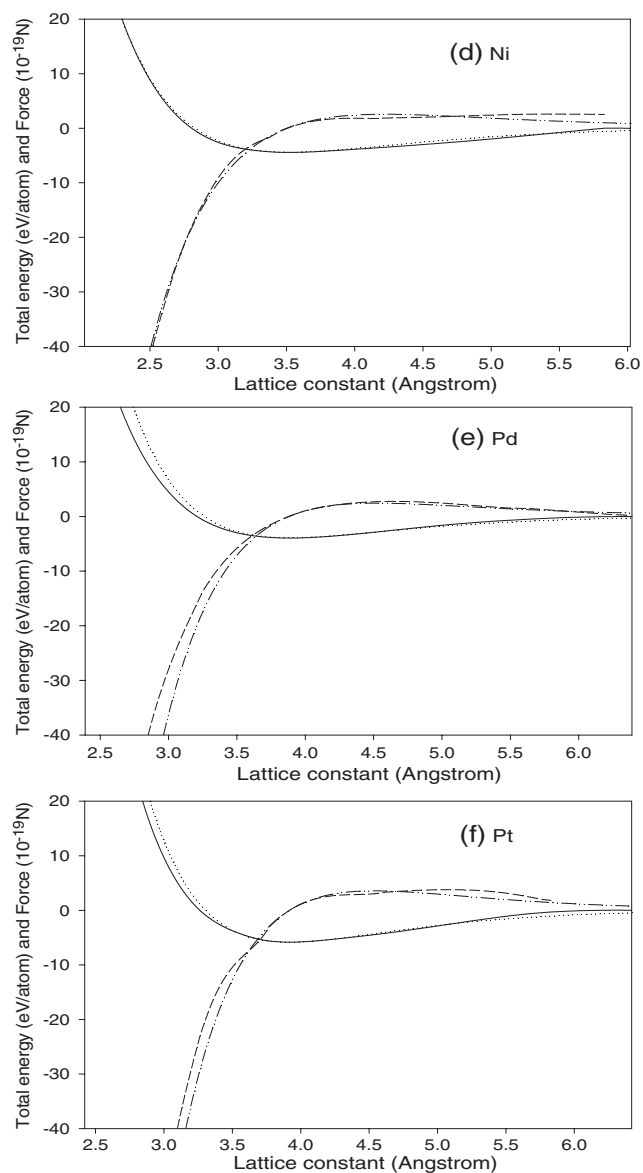
Figure 3. (Continued.)

It is clear that the agreement between the calculated results and experimental values is good. The above results suggest that the proposed extended FS potential could also overcome the 'soft' behaviour for fcc metals, as it moves away from the equilibrium state. It is therefore deduced that the proposed extended FS potential can be used in atomistic simulation for fcc metals, even if some volume–pressure change may emerge.

4.3. Melting point and melting heat

Using the same method as mentioned in section 3.3, the melting points and the melting heats of the six selected fcc metals are also monitored based on their extended FS potentials. The
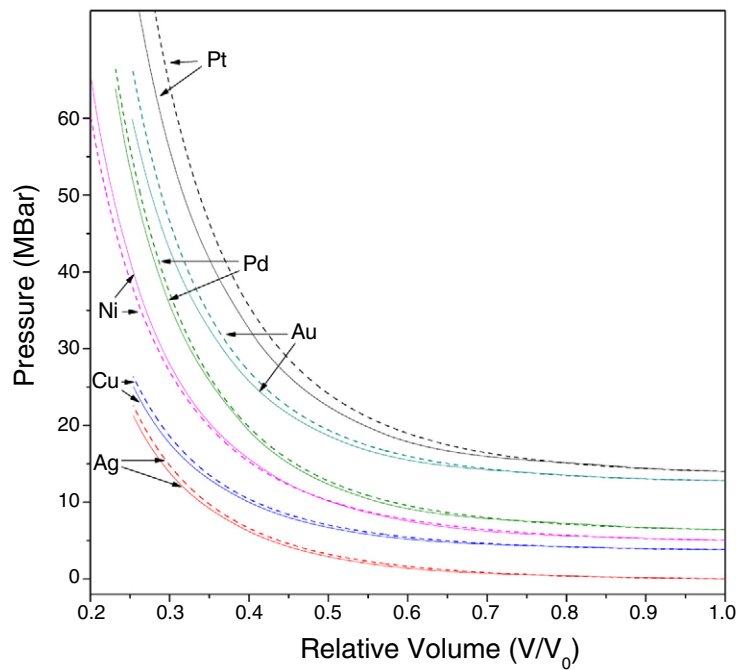
Figure 4. The pressure versus volume relationships for six fcc metals, i.e. Cu, Ag, Au, Ni, Pd and Pt. The solid curves are from extended FS potentials, and the dashed curves are from the Rose equation.
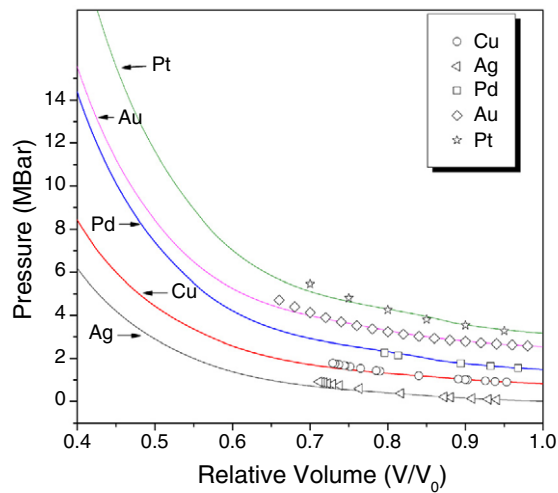
Figure 5. The pressure versus volume relationships for six fcc metals, i.e. Cu, Ag, Au, Ni, Pd and Pt. The solid curves are from extended FS potentials, and the scattered dots are from experiments. (Cu, Ag and Pd are from [33], Au is from [34], and Pt is from [35].)

simulated values together with their corresponding experimental values are all listed in table 5. One sees from the table that the calculated melting points of Cu, Ag, Ni and Pd are in good agreement with the experimental values, as the maximum error for Cu, Ag, Ni and Pd is less

Table 5. The melting points and melting heats for six selected fcc metals. The experimental data are from [19].

		Cu	Ag	Au	Ni	Pd	Pt
Melting point	MD	1300	1175	1475	1800	1875	2225
(K)	Expt	1358	1235	1337	1728	1828	2042
Melting heat	MD	9.16	8.95	13.14	13.74	16.60	16.37
(kJ mol^{-1})	Expt	13.05	11.30	12.55	17.47	17.60	19.60

than 5%, and that the maximum errors in the calculated melting points for Pt and Au are 8.8 and 10.3%, respectively. For melting heats, the calculated values are reasonably compatible with the experimental values, with a maximum error of about 31.6%. Apparently, the extended FS potential can also reasonably reflect the thermodynamic properties of fcc metals.

5. Application for fcc–bcc systems

In the present section, we will show that the extended FS potential can also be successfully applied to some fcc–bcc systems. We present here the results obtained from the four equilibrium immiscible Ag–refractory metal systems, i.e. Ag–Mo, Ag–Nb, Ag–Ta and Ag–W systems, characterized by relatively large positive heats of formation, being +56, +25, +23 and +65 kJ mol^{-1}, respectively [36].

5.1. Construction of the cross potentials

For fcc–bcc cross potentials, the forms expressed by equations (1)–(5) are also adopted. It is known that for equilibrium immiscible systems it is a challenging task to fit the cross potentials, as there are no available experimental data related to the respective alloy compounds. In this respect, the first-principles calculation based on quantum mechanics is known to be a reliable way to acquire some physical properties of some possible intermetallic compounds [37–39]. In the present study, the first-principles calculations are carried out using the well established Vienna *ab initio* simulation package (VASP) [40, 41]. In the calculation, the plane-wave basis and fully nonlocal Vanderbilt-type ultrasoft pseudo-potentials are employed [42]. The exchange and correlation items are described by the generalized-gradient approximation (GGA) proposed by Perdew and Wang [43]. The integration in the Brillouin zone is done in a mesh of $11 \times 11 \times 11$ special k points determined according to the so-called Monkhorst–Pack scheme, as such integration is proved to be sufficient for the computation of the simple structures [44]. Through *ab initio* calculations, the lattice constants and cohesive energies of some hypothetic Ag–Mo(Nb, Ta, W) alloys are obtained and then applied in fitting the Ag–Mo(Nb, Ta, W) cross potentials. The parameters of the fitted Ag–Mo(Nb, Ta, W) cross potentials are listed in table 6. Based on the constructed extended FS potentials, the lattice constants and cohesive energies of some hypothetical compounds in the four Ag–refractory metal systems are calculated and the results are listed in table 7. For comparison, the results deduced directly from *ab initio* calculations are also listed in the table. From table 7, one sees clearly that the reproduced values are in good agreement with those from *ab initio* calculations, suggesting that extended FS potential is reasonable to describe the atomic interactions in the Ag–refractory metal systems.

Table 6. Fitted parameters for Ag–Mo(Nb, Ta, W) cross potentials.

	Ag–Mo	Ag–Nb	Ag–Ta	Ag–W
A (eV Å^{-1})	0.5452	0.3963	0.8331	0.6962
d (Å)	4.30	4.20	4.36	4.60
c (Å)	4.40	4.50	4.50	4.30
c_0 (eV Å^{-2})	29.0724	46.2206	37.9635	25.6180
c_1 (eV Å^{-3})	−29.2625	−45.5157	−37.9588	−26.3407
c_2 (eV Å^{-4})	9.8921	15.0141	12.7381	9.1414
c_3 (eV Å^{-5})	−1.1251	−1.6656	−1.4352	−1.0693
c_4 (eV Å^{-6})	0	0	0	0
B (Å^{-2})	0	0	0	0

Table 7. The lattice constants and cohesive energies of some Ag–Mo, Ag–Ta, Ag–Nb and Ag–W alloys.

Compounds		a (Å)	E_c (eV)	Compounds		a (Å)	E_c (eV)
Ag$_3$Mo L1$_2$	This work	4.13	3.1166	Ag$_3$Nb L1$_2$	This work	4.20	3.5350
	VASP	4.13	3.1166		VASP	4.20	3.5352
AgMo B2	This work	3.23	3.9161	AgNb B2	This work	3.32	4.7237
	VASP	3.23	3.9161		VASP	3.32	4.7233
AgMo$_3$ L1$_2$	This work	3.99	5.2072	AgNb$_3$ L1$_2$	This work	4.18	6.3226
	VASP	3.99	5.4438		VASP	4.17	6.1628
Ag$_3$Ta L1$_2$	This work	4.18	3.5970	Ag$_3$W L1$_2$	This work	4.13	3.4291
	VASP	4.18	3.5962		VASP	4.13	3.4542
AgTa B2	This work	3.30	4.9048	AgW B2	This work	3.22	4.7990
	VASP	3.30	4.9060		VASP	3.22	4.7212
AgTa$_3$ L1$_2$	This work	4.17	6.5297	AgW$_3$ L1$_2$	This work	4.01	6.7903
	VASP	4.17	6.5288		VASP	4.01	6.8686

5.2. Elastic constants of alloys

For the four Ag–refractory metal systems, we reproduce the elastic constants of some possible alloys at a few specific compositions, based on the newly constructed extended FS potentials of the systems. For comparison, the well known *ab initio* program CASTEP [45] is also employed to acquire the elastic constants. In CASTEP calculations, the nonlocal ultrasoft pseudo-potentials have also been used, together with a kinetic energy cut-off of 330 eV and the PW91 GGA exchange–correlation functional. A $15 \times 15 \times 15$ special *k*-point sampling mesh of the Brillouin zone is found to produce converged results for all cubic structures, while for the D0$_{19}$ structure the mesh is set to $9 \times 9 \times 9$. In table 8, the elastic constants calculated by the extended FS potential and from CASTEP, respectively, are listed. From the table, one sees that the signs of the results derived by the extended FS potential and CASTEP, respectively, are quite consistent with each other, though some of the values have some discrepancy. From the data listed in the table, one could also see some unusual features in the elastic behaviour. First, the elastic constants $C' = (C_{11} - C_{12})/2$ of the B2 AgTa, L1$_2$Ag$_3$W, L1$_2$Ag$_3$Mo, and B2 AgNb alloys are negative, implying that these structures are dynamically unstable under an elastic shearing. Second, in all the other cases, the C_{44} and C' are all positive, suggesting that these structures may elastically be stable. The qualitative agreement between the reproduced values

Table 8. The elastic constants (the unit is GPa) of the Ag–Mo(Nb, Ta, W) alloys.

Compounds			a (Å)	c (Å)	C_{11}	C_{12}	C_{13}	C_{33}	C_{44}	C'
Ag$_3$Ta	D0$_{19}$	CASTEP	2.94	4.62	168.75	135.33	87.00	260.38	42.87	16.71
		This work	2.96	4.82	119.07	59.25	49.91	133.48	20.38	29.91
AgTa$_3$	D0$_3$	CASTEP	6.50		240.85	180.36			97.59	30.24
		This work	6.73		124.77	123.30			67.93	0.73
AgTa	B2	CASTEP	3.25		152.34	191.55			84.89	−19.60
		This work	3.30		167.12	180.33			133.04	−6.60
Ag$_3$W	L1$_2$	CASTEP	4.16		95.50	125.20			22.59	−14.84
		This work	4.13		15.35	66.83			33.73	−25.74
AgW$_3$	D0$_{19}$	CASTEP	2.99	4.60	133.21	95.13	100.70	320.54	57.32	19.03
		This work	2.80	4.56	242.85	105.81	73.91	266.98	36.12	68.52
AgW$_3$	L1$_2$	CASTEP	4.08		261.57	202.90			138.10	29.33
		This work	3.96		139.74	138.93			101.97	0.40
Ag$_3$Mo	L1$_2$	CASTEP	4.11		120.11	124.08			38.99	−1.98
		This work	4.13		3.37	76.05			45.63	−36.33
Ag$_3$Mo	D0$_3$	CASTEP	6.48		135.43	133.69			88.67	0.868
		This work	6.84		54.28	48.54			19.05	2.87
AgMo$_3$	D0$_{19}$	CASTEP	2.86	4.55	236.63	139.68	126.05	357.39	69.22	48.47
		This work	2.82	4.59	174.94	82.03	51.03	200.29	14.35	46.45
Ag$_3$Nb	L1$_2$	CASTEP	4.16		119.05	114.08			41.12	2.48
		This work	4.20		132.00	92.42			63.47	19.78
Ag$_3$Nb	D0$_{19}$	CASTEP	2.97	4.63	149.21	133.09	81.31	238.31	41.23	8.05
		This work	2.97	4.84	176.52	78.18	65.03	195.83	35.02	49.16
AgNb	B2	CASTEP	3.30		115.94	165.79			69.58	−24.92
		This work	3.32		185.75	280.80			204.64	−47.52

and those from CASTEP calculations suggests that the extended FS potential can reasonably describe the elastic behaviour in the equilibrium immiscible Ag–refractory metal systems.

6. Concluding remarks

Through enhancing the repulsive interaction, the proposed extended FS potential performs well in reflecting the pressure–volume relationship for bcc metals and is capable of reproducing some basic physical properties of fcc metals, thus overcoming the shortcoming of the original FS formalism.

The proposed extended FS potential is also good at deriving the equations of state for some bcc and fcc metals, which are in good agreement with the Rose equation, indicating the extended FS potential can reasonably describe the energy and force even when the distance is far from the equilibrium state.

The proposed extended FS potential is also able to correctly reproduce the lattice constants, cohesive energies and elastic constants of some possible compounds in the Ag–refractory metal systems, indicating that the potential is capable of describing the interactions in fcc–bcc systems.

Acknowledgments

References

[1] Gupta R P 1981 *Phys. Rev.* B **23** 6265
[2] Daw M S and Baskes M I 1984 *Phys. Rev.* B **29** 6443
[3] Jacobsen K W, Norskov J K and Puska M J 1987 *Phys. Rev.* B **35** 7423
[4] García-Rodeja J, Rey C, Gallego L J and Alonso J A 1994 *Phys. Rev.* B **49** 8495
[5] Tomanek D, Aligia A A and Balseiro C A 1985 *Phys. Rev.* B **32** 5051
[6] Daw M S and Baskes M I 1983 *Phys. Rev. Lett.* **50** 1285
[7] Finnis M W and Sinclair J E 1984 *Phil. Mag.* A **50** 45
[8] Maysenhoelder W 1986 *Phil. Mag.* A **53** 783
[9] Yan M, Vitek V and Chen S P 1996 *Acta Mater.* **44** 4351
[10] Koleske D D and Sibener S J 1993 *Surf. Sci.* **290** 179
[11] Landa A, Wynblatt P, Girshich A, Vitek V, Ruban A and Skriver H 1988 *Acta Mater.* **46** 3027
[12] Zhang Q, Lai W S and Liu B X 1998 *Phys. Rev.* B **58** 14020
[13] Rebonato R, Welch D O, Hatcher R D and Bilello J C 1987 *Phil. Mag.* A **55** 655
[14] Ackland G J and Thetford R 1987 *Phil. Mag.* A **56** 15
[15] Rose J H, Smith J R, Guinea F and Ferrante J 1984 *Phys. Rev.* B **29** 2963
[16] Ackland G J, Tichy G, Vitek V and Finnis M W 1987 *Phil. Mag.* A **56** 735
[17] Johnson R A 1988 *Phys. Rev.* B **37** 3924
[18] Kittel C 1996 *Introduction to Solid State Physics* 7th edn (New York: Wiley)
[19] Lide David R 2000–2001 *Handbook of Chemistry and Physics* 81st edn (Boca Raton, FL: CRC Press)
[20] Schepper L D, Segers D, Dorikens-Vanpraet L, Dorikens M, Knuyt G, Stals L M and Moser P 1983 *Phys. Rev.* B
       27 5257
[21] Janot C, George B and Delcroix P 1982 *J. Phys. F: Met. Phys.* **12** 47
[22] Maier K, Peo M, Saile B, Schaefer H E and Seeger A 1979 *Phil. Mag.* A **40** 701
[23] Miedema A R 1979 *Z. Metallkd.* **79** 345
[24] Lee B J, Bakes M I, Kim H and Cho Y K 2001 *Phys. Rev.* B **64** 184102
[25] Hyunchae C and Choong-Shik Y 1999 *Phys. Rev.* B **59** 8526
[26] Hixson R S and Fritz J N 1992 *J. Appl. Phys.* **71** 1721
[27] Li J H, Kong L T and Liu B X 2004 *J. Mater. Res.* **19** 3547
[28] Cohen E R, Lide D R and Trigg G L 2003 *AIP Physics Desk Reference* 3rd edn (New York: AIP Press)
[29] Balluffi R W 1978 *J. Nucl. Mater.* **69/70** 240
[30] Wycisk W and Feller-Knipmeier M 1978 *J. Nucl. Mater.* **69/70** 616
[31] Foiles M, Baskes M I and Daw M S 1986 *Phys. Rev.* B **33** 7983
[32] Cai J and Ye Y Y 1996 *Phys. Rev.* B **54** 8398
[33] Mao H K, Bell P M, Shaner J W and Steinberg D J 1978 *J. Appl. Phys.* **49** 3276
[34] Anderson O L, IsaaK D G and Yamamoto S 1989 *J. Appl. Phys.* **65** 1534
[35] Holmes N C, Moriaty J A, Gathers G R and Nellis W J 1989 *J. Appl. Phys.* **66** 2962
[36] Boer F R D, Boom R, Mattens W C M, Miedema A R and Niessen A K 1988 *Cohesion in Metals–Transition
       Metal Alloys* (Amsterdam: North-Holland)
[37] Luzzi D E, Yan M, Šob M and Vitek V 1991 *Phys. Rev. Lett.* **67** 1894
[38] Yan M, Šob M, Luzzi D E, Vitek V, Ackland G J, Methfessel M and Rodriguez C O 1993 *Phys. Rev.* B **47** 5571
[39] Siegl R, Yan M and Vitek V 1997 *Modelling Simul. Mater. Sci. Eng.* **5** 105
[40] Kresse G and Hafner J 1993 *Phys. Rev.* B **47** 558
[41] Kresse G and Furthmuller J 1996 *Phys. Rev.* B **54** 11169
[42] Vanderbilt D 1990 *Phys. Rev.* B **41** 7892
[43] Perdew J and Wang Y 1992 *Phys. Rev.* B **45** 13244
[44] Liu J B and Liu B X 2001 *Phys. Rev.* B **63** 132204
[45] Segall M D, Lindan P L, Probert M J, Pickard C J, Hasnip P J, Clark S J and Payne M C 2002 *J. Phys.: Condens.
       Matter* **14** 2717